

Is There an Association Between Olfactory Bulb Volume and the Keros Type of Fossa Olfactoria?

Muzaffer Saglam, MD,* Murat Salihoglu, MD,† Hakan Tekeli, MD,‡ Aytug Altundag, MD,§
Ali Kemal Sivrioglu, MD,|| and Melih Cayonu, MD¶

Purpose: The purpose of this study was to investigate the relationship between the volume of the olfactory bulb (OB), the depth of the olfactory sulcus (OS), the depth of the fossa olfactoria (FO), and the height of the OB.

Methods: A total of 54 patients participated (9 women and 45 men; mean [SD] age, 27 [38] y; range, 20–45 y). Magnetic resonance imaging was performed with a 1.5-T system (slice thickness, 1 mm). Measurements of the right and left OB volumes were performed through manual segmentation of the coronal slices. We measured the depth of the FO on the basis of Keros classification on coronal magnetic resonance images. The depth of the OS was measured on the coronal plane at the posterior tangent through the orbital globes. The height of the OB was measured on the coronal plane of the cribriform plate at the highest portion of the OB.

Results: The mean (SD) right OB volume was measured to be 52.21 (13.73) mm³ with a range between 33.90 and 95.70 mm³. The mean (SD) left OB volume was measured to be 53.98 (13.31) mm³ with a range between 31.20 and 94.10 mm³. Type 1, type 2, and type 3 Keros ratios of the FO bilaterally were 12.9% (7/54), 68.5% (37/54), and 3.7% (2/54), respectively. There was no significant relationship between the OB volume and ipsilateral Keros type of FO (right side: $P = 0.208$; left side: $P = 0.164$). Similarly, there was no significant relationship between the OB volume and depth of OS on both sides (right side: $P = 0.073$; left side: $P = 0.065$). There was no significant association between the Keros type of the right FO and depth of the OS (right side: $P = 0.812$; left side: $P = 0.863$).

Conclusions: We conclude that there is no statistical correlation between the OB volume and depth of the FO (Keros type). From the current study, it may be concluded that the depth of the FO may develop largely independent from OB volumes. The individuals without smell disorder have a wide range in OB volume. The method of OB volume measurement that we described is a valid measure of real OB volumes with high reproducibility.

Key Words: Fossa olfactoria, Keros classification, magnetic resonance imaging, olfactory bulb volume, olfactory sulcus

(*J Craniofac Surg* 2014;25: 1273–1276)

Studies about the olfactory bulb (OB) have recently received public interest. The OB lies just above the cribriform plate in the fossa olfactoria (FO). It continues with the olfactory tract (OT) and is closely related to the olfactory sulcus (OS) of the frontal lobe. The OB is considered a plastic structure. Many congenital anomalies, brain or sinus surgery, and head trauma may effect or change the OB volume. The depth of FO was divided into 3 types by Keros in 1962.¹ In Keros type 1, the FO is 1- to 3-mm deep, the lateral lamella is short, and the ethmoid roof is almost in the same axial plane as the cribriform plate. In Keros type 2, the FO is 4- to 7-mm deep. In Keros type 3, the FO is 8- to 16-mm deep and the ethmoid roof lies significantly above the cribriform plate. In fetal life, the skull base consists primarily of cartilage. From fetal life to the first year of age, the ethmoid bone consists of 2 separate symmetric halves that join by the end of the first year of life. Most cartilages of the anterior skull base have ossified at the end of 2 years of life.^{2,3}

Factors relating to the development of depth of the FO are not well understood. In this study, we investigated the possible relation between the development of depth of the FO, the volume of the OB, the depth of the OS, and the height of the OB.

MATERIALS AND METHODS

Participants

The institutional ethics committee approved this retrospective study (no. 2012-42, GATA Haydarpaşa Teaching Hospital, Istanbul, Turkey). A total of 54 patients participated (9 women and 45 men; mean [SD], age, 27 [38] y; range, 20–45 y). Patients who had brain volume loss due to previous infarction, surgery, trauma, residual hemorrhage in the frontal lobes and anteroinferior temporal lobes, chronic rhinosinusitis, smell disorder, multiple sclerosis, and older than 45 years were excluded. Patients' complaints are listed in Table 1.

Magnetic Resonance Imaging

All examinations were performed on a 1.5-T magnetic resonance imaging (MRI) system (Avanto; Siemens, Erlangen, Germany) using a 12-channel head coil. Sections were angulated perpendicular to the anterior base of skull or cribriform plate. We used three-dimensional T2 short-term inversion recovery (STIR) sampling perfection with application optimized contrast using different flip angle evolutions (SPACE) covering the anterior and middle segments of the base of the skull. Parameters of the three-dimensional T2 STIR SPACE sequence were as follows: echo time, 224 milliseconds; repetition time, 1440 milliseconds; bandwidth, 350 hertz per pixel;

From the Departments of *Radiology, †Otorhinolaryngology, ‡Neurology, GATA Haydarpaşa Teaching Hospital; §Department of Otorhinolaryngology, Istanbul Surgery Hospital, Istanbul; ||Department of Radiology, Aksaz Military Hospital, Muğla; and ¶Department of Otorhinolaryngology, Amasya University Training and Research Hospital, Amasya, Turkey. Received September 24, 2013.

Accepted for publication November 14, 2013.

Address correspondence and reprint requests to Muzaffer Saglam, MD, Department of Radiology, GATA Haydarpaşa Teaching Hospital, Uskudar, Istanbul, 34668, Turkey; E-mail address: msaglam@gata.edu.tr

The authors report no conflicts of interest.

Copyright © 2014 by Mutaz B. Habal, MD

ISSN: 1049-2275

DOI: 10.1097/SCS.0000000000000579

TABLE 1. Patients' Complaints

Symptoms	No. Patients	%
Headache	29	53.7
Dizziness	9	16.6
Tinnitus	5	9.2
Prolactinoma	4	7.4
Peripheral facial paralysis	4	7.4
Sleep apnea	3	5.5

field of view, 190 × 190; matrix, 520 × 512; slice thickness, 1 mm; interslice gap, 0.

Syngo MMWP software was used to determine the volume of the right and left OBs. Volume measurements were performed by an experienced radiologist blinded to the clinical diagnosis. Before volumetric measurement, a midsagittal image of the OB was chosen and the length of both OBs was measured (Fig. 1). Afterward, the measurements of the right and left OB volumes were performed through manual segmentation of the coronal slices by planimetric manual contouring (surface in pixels), then all pixels were added and multiplied by the x, y, and z axes (0.36 × 0.37 × 1 number of pixels) to obtain a volume in cubic millimeters (Fig. 2).

When determining the caudal border of the OB, we used sagittal images to detect the most caudal fila olfactoria. We accepted the portion beyond this point as OT. In some cases in which we could not clearly determine the fila olfactoria, we used the cribriform plate as an additional anatomic landmark that is typically seen as a smooth depression on the surface of the anterior base of skull. The posterior border of this depression is also helpful for identifying the posterior border of the OB (Fig. 3). In addition, in cases where we could not clearly detect the fila olfactoria and the posterior border of the cribriform plate, we used the method that has previously been described by Yousem et al⁴ and Rombaux et al.⁵ Here, the posterior border of the OB was determined as the slice where the OB changes from a round to an oval shape in combination with a change in caliber. Apart from the three-dimensional T2 STIR SPACE sequence, fluid-attenuated inversion recovery (FLAIR) and contrast-enhanced T1 sequences were

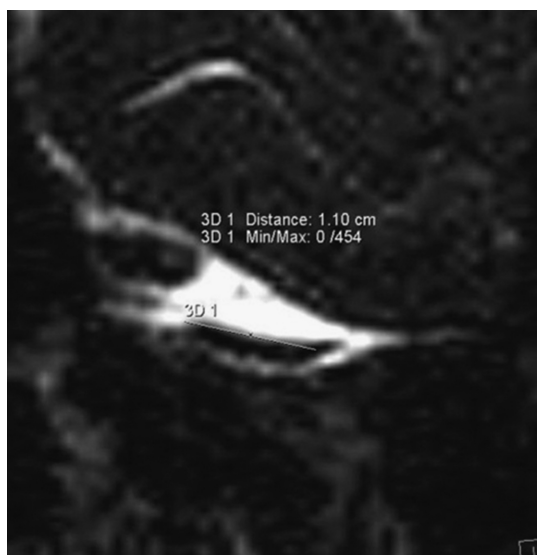


FIGURE 1. Three-dimensional T2 STIR SPACE midsagittal image of the OB clearly delineates the OB and fila olfactorias (arrows). The length of the OB was measured 11 mm.

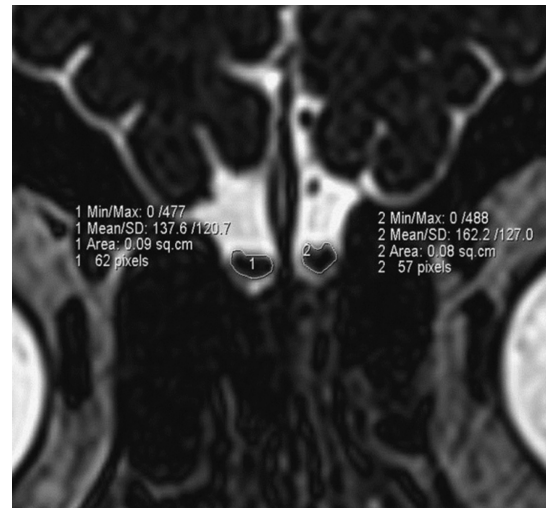


FIGURE 2. Measurement of the surface area of both OBs in a patient on coronal three-dimensional T2 STIR SPACE image.

used for detecting any abnormal signal and enhancement in the OB whenever deemed necessary.

We measured the depth of the FO on the basis of Keros classification on coronal MRI images (Fig. 4). The Keros classification depends on the length of the lateral lamella of the cribriform plate. We used the coronal images for identifying the Keros type of the FO. The depth of the OS was measured on the coronal plane of the posterior tangent through the eyeballs. A straight line tangent to the surface of the top of the gyrus rectus and to that of the orbital gyrus is drawn at first, and the depth of the OS is measured by drawing a perpendicular line connecting this tangent line to the deepest point of the sulcus. The depth of the OS is measured by drawing a perpendicular line to the deepest point of the sulcus. The height of the OB was measured on the coronal plane of the cribriform plate at the highest portion of the OB.

Statistical Analysis

The defining statistics related to the characteristics of interest were expressed as mean, standard deviation, as well as minimum and maximum values. Distribution of the data for right-left OB volume

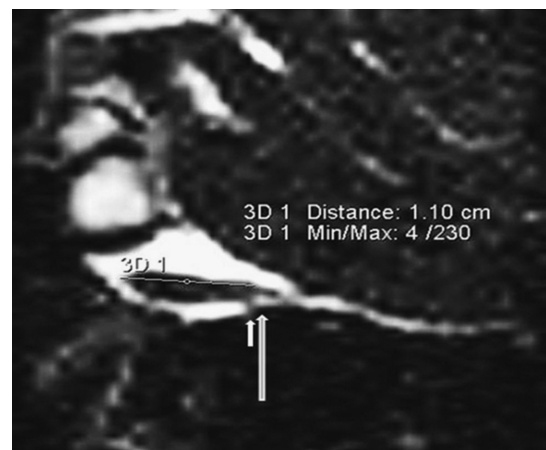


FIGURE 3. Midsagittal image of the OB. Dorsal fila olfactoria is seen as a vertical hypointensity (arrow). Posterior border of the smooth depression of the cribriform plate is marked by long arrow. The length of the OB was measured 11 mm.

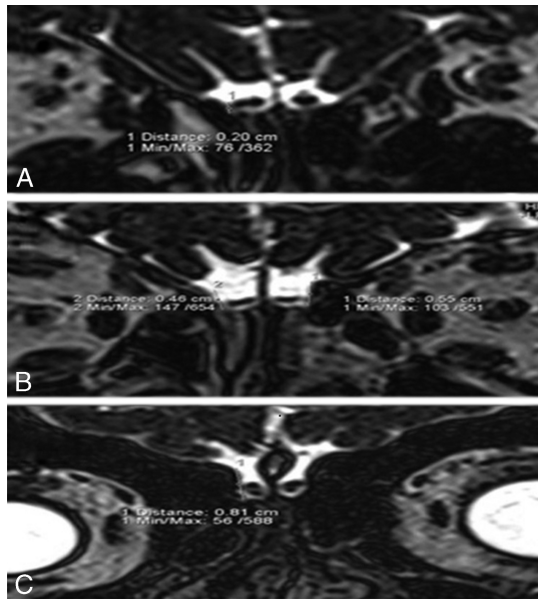


FIGURE 4. Coronal three-dimensional T2 STIR SPACE images show Keros 1 (A), Keros 2 (B), and Keros 3 (C) type of the FO consecutively.

and right-left depth of the OS was homogenous according to the Kolmogorov-Smirnov test. However, normal distribution was not observed for both heights of the OB. The Pearson correlation test was used to investigate the distribution of the data of bilaterally OB volumes and the depth of the OS. The analysis of variance test was used to investigate the statistical relation between the Keros type of the FO and OB volume as well as the depth of the OS. The repeatability of the 2 measurements was evaluated using the interclass correlation coefficient. The α level was set at 0.05. All statistical analyses were performed using Statistical Package for the Social Sciences 15.0 for Windows (SPSS Inc, Chicago, IL) and Medcalc 9.3.9.0 (MedCalc Software, Ostend, Belgium).

RESULTS

On MRI, we found 1 Chiari malformation type 1 in a patient with headache, 1 high jugular bulb in a patient with tinnitus, 3 pituitary microadenomas, and 1 pathologic enhancement of the mastoid portion of the facial nerve in a patient with facial paralysis. The rest of the MRIs were normal without any abnormalities at the anterior skull base or olfactory area. Descriptive statistics of both OB volumes, depths of OS, and heights of OB are shown in Table 2. The mean (SD) right OB volume was measured 52.21 (13.73) mm³ with a range of minimum 33.90 mm³ and maximum 95.70 mm³. The mean (SD) left OB volume was measured 53.98 (13.31) mm³ with a range of minimum 31.20 and maximum 94.10 mm³. Type 1, type 2, and type 3 Keros ratios of the FO bilaterally were 12.9% (7/54), 68.5% (37/54), and 3.7% (2/54), respectively. Eight cases (14.8%) presented with asymmetric Keros type.

There was no significant relationship between the OB volume and ipsilateral Keros type of the FO (right side: $P = 0.208$; left side: $P = 0.164$). Similarly, there was no significant relationship between the OB volume and depth of the OS at both sides (right side: $P = 0.073$; left side: $P = 0.065$).

There was no significant association between the Keros type of the right FO and right and left depth of the OS (right side: $P = 0.812$; left side: $P = 0.863$). There was a statistically significant relationship and moderate correlation between the right OB volume and bilateral height of the OBs (bilateral: $P = 0.025$, $r = 0.306$). However, a statistically significant relationship was not observed between the left OB volume and ipsilateral and contralateral height of the OB (ipsilateral: $P = 0.053$; contralateral: $P = 0.206$).

When both OB volumes were studied at different times by the same radiologist, it was found that the repeatability of the measurements was excellent (interclass correlation coefficient of 0.99 for both OB volumes).

DISCUSSION

The OB is an oval-shaped true neocerebral structure. Both OBs occupy the most anterior portion of the skull base and lie on the cribriform plate in the FO. After birth, progressive reorganization of the peripheral neuronal layers and signal intensity changes of the central area of the OB are seen. These changes are completed at the end of the second year, paralleling cerebral maturational changes. Magnetic resonance imaging has been used successfully to reflect these changes.⁶ We performed the three-dimensional T2 STIR SPACE sequence for volume and distance measurements because the SPACE sequence provides high contrast between fluid and other structures such as the OB, OT, and other peripheral nerves with high-spatial resolution imaging.⁷ The OB is considered a plastic structure because its volume may be affected by many congenital variations, disease, surgery, or trauma.

Keros classification is generally assessed on coronal images. Although this is traditionally identified on computed tomographic (CT) imaging, we used MRI for its soft tissue resolution. We found that MRI has enough resolution quality to determine the Keros type of the FO without the need for paranasal CT imaging. Factors contributing to the depth of the FO are not well understood, although there is information on how the anterior skull base develops. The anterior skull base is largely cartilaginous at birth. The first ossification is detected in the roof of the ethmoidal labyrinth laterally, and ossification spreads toward the midline. Half of the anterior skull base has completely ossified at 6 months of age. Ossification steadily increases over the first 2 years of life. At 2 years of age, the anterior skull base is completely ossified, with a cartilaginous gap anteriorly in the region of the foramen cecum, the residual unossified portion.^{2,3} The fovea ethmoidalis of the frontal bone separates the ethmoidal cells from the anterior cranial fossa. The very thin horizontal cribriform plate of the ethmoid bone is bounded laterally by the vertical lateral lamella. The lateral lamella is located between the cribriform plate and the fovea ethmoidalis and is the thinnest bone in the entire anterior skull base. It is well-known that longer lateral lamellae pose greater risks for intracranial entry during

TABLE 2. Descriptive Statistics of Both OB Volumes, Depth of Both OS and Height of Both OB

N = 54	Right OB Volume (mm ³)	Left OB Volume (mm ³)	Right OS Deepness (mm)	Left OS Deepness (mm)	Right OB Height (mm)	Left OB Height (mm)
Mean	52.21	53.98	7.33	7.35	—	—
Median	—	—	—	—	1.8	1.8
Std. Deviation	13.73	13.31	1.62	1.56	—	—
Minimum	33.9	31.2	4	4	1.4	1.4
Maximum	95.7	94.1	11	11	3.2	3.2

surgery.^{8,9} So, it is very important for ear, nose, and throat surgeons to know Keros type of the FO with paranasal sinus CT before surgery. The space between the cribriform plate, lateral lamella, and medially located perpendicular plate is named as FO. It is seen as a variable depression in the cribriform plate that contains the olfactory nerve and a small artery. Interestingly, the shapes of the skull base, calvarial bone, and the adjacent neural structures seem to be complementary to each other. In healthy subjects without smell disorder, the OB has a wide range in volume.¹⁰ The current study supports this variation in OB volume, too. Thus, we propose that children younger than 2 years might have the same individual variation in OB volume, too. Depending on this, we speculated that the OB might play a role in the formation of FO. However, a relationship between a bony structure (ossified by the age of 2 y) and a highly plastic structure was questionable. Contrary to our prediction, we could not find a statistically significant relation between the OB volume and depth of the FO.

Our study has some limitations. First, our study group consists of only young adults and we have no data from infants and children. Second, we used three-dimensional T2 STIR SPACE sequence for identifying the OB and making the volumetric measurement. Keros classification was based on these coronal magnetic resonance images. It is known that osseous anatomy of the skull base is well depicted by CT. However, in our study, MRI had enough resolution to determine the Keros type of the FO without the need for paranasal CT imaging. Third, we used the three-dimensional T2 STIR SPACE sequence for the measurements of OB volume. Pathologic signal changes are easily seen on T2, FLAIR, and contrast-enhanced T1 sequences. We used SPACE sequence because of its high spatial resolution and three-dimensional imaging properties. In addition to this sequence, whenever indicated, we also performed T2, FLAIR, and contrast-enhanced T1 sequences to detect any signal abnormality in the OB.

CONCLUSIONS

We conclude that there is no statistical correlation between the OB volume and depth of the FO. From the current study, it may be carefully concluded that the depth of the FO may develop largely independent from OB volumes. Future studies during the prenatal

period and postnatal 2-year period are needed to understand the factors that affect the development of the FO. Individuals without smell disorders have a wide range in OB volume. The method of OB volume measurement that we described is a valid measure of real OB volumes with high reproducibility.

ACKNOWLEDGMENT

The authors thank Thomas Hummel for his helpful comments on previous manuscript versions of this article.

REFERENCES

1. Keros P. On the practical value of differences in the level of the lamina cribrosa of the ethmoid [in German]. *Z Laryngol Rhinol Otol* 1962;41:808–813
2. Scott JH. The cartilage of the nasal septum (a contribution to the study of facial growth). *Br Dent J* 1953;95:37–43
3. Belden CJ, Mancuso AA, Kotzur IM. The developing anterior skull base: CT appearance from birth to 2 years of age. *AJNR Am J Neuroradiol* 1997;18:811–818
4. Yousem DM, Geckle RJ, Doty RL, et al. Reproducibility and reliability of volumetric measurements of olfactory eloquent structures. *Acad Radiol* 1997;4:264–269
5. Rombaux P, Grandin C, Duprez T. How to measure olfactory bulb volume and olfactory sulcus depth? *B-ENT* 2009;5:53–60
6. Schneider JF, Floemer F. Maturation of the olfactory bulbs: MR imaging findings. *AJNR Am J Neuroradiol* 2009;30:1149–1152
7. Viallon M, Vargas MI, Jlassi H, et al. High-resolution and functional magnetic resonance imaging of the brachial plexus using an isotropic 3D T2 STIR (short term inversion recovery) SPACE sequence and diffusion tensor imaging. *Eur Radiol* 2008;18:1018–1023
8. Stammberger HR, Kennedy DW, The Anatomic Terminology Group. Paranasal sinuses: anatomic terminology and nomenclature. *Ann Otol Rhinol Laryngol Suppl* 1995;167:7–16
9. Gauba V, Saleh GM. Radiological classification of anterior skull base anatomy prior to performing medial orbital wall decompression. *Orbit* 2006;25:93–96
10. Rombaux P, Duprez T, Hummel T. Olfactory bulb volume in the clinical assessment of olfactory dysfunction. *Rhinology* 2009;47:3–9